

## Continuum and lattice heat currents for oscillator chains

Onuttom Narayan and A. P. Young

*Department of Physics, University of California, Santa Cruz, California 95064, USA*

(Received 2 March 2009; published 7 July 2009)

We show that two commonly used definitions for the heat current give different results—through the Kubo formula—for the heat conductivity of oscillator chains. The difference exists for finite chains, and is expected to be important more generally for small structures. For a chain of  $N$  particles that are tethered at the ends, the ratio of the heat conductivities calculated with the two currents differs from unity by  $O(1/N)$ . For a chain held at constant pressure, the difference from unity decays more slowly, and is consistent with  $O(1/N^\eta)$  with  $1 > \eta > 0.5$ .

DOI: [10.1103/PhysRevE.80.011107](https://doi.org/10.1103/PhysRevE.80.011107)

PACS number(s): 05.60.Cd, 44.10.+i, 05.70.Ln

### I. INTRODUCTION

In linear-response theory, transport currents that flow in a system in response to small gradients in thermodynamic potentials are calculated in terms of equilibrium autocorrelation functions of these currents through the Green-Kubo formula [1]. This involves taking the thermodynamic limit of the autocorrelation functions first, and then the zero-frequency limit; the order in which the limits are taken is important [2]. The response function to be calculated determines the appropriate correlation function: for instance, the electric and thermal conductivities involve the autocorrelation functions of the particle and heat currents, respectively.

Unlike the particle current, which is defined unambiguously, there are many possible choices for the energy current, and therefore the heat current which is a linear combination of the two [3]. Most notably, the heat current can be defined in the continuum or on a lattice; both are commonly used. For the lattice current, the energy of each particle is assigned to the lattice site associated with the particle. This is commonly used for oscillator chains, and seems reasonable for crystals (if we neglect lattice defects). The energy current flowing from the lattice site  $i$  to  $k$  is

$$j_{ik} = \frac{1}{2} \mathbf{F}_{ik} \cdot (\mathbf{v}_i + \mathbf{v}_k), \quad (1)$$

where  $\mathbf{F}_{ik}$  is the force exerted on the  $k$ th particle by the  $i$ th particle, and  $\mathbf{v}_{i,k}$  are the velocities of the particles. For the continuum current, commonly used for hard-particle systems or fluids, the energy of each particle resides at its instantaneous location. As a result, there is an advective part to the energy current from the motion of particles

$$\mathbf{j}_{\text{adv}}(\mathbf{x}) = \sum_i e_i \mathbf{v}_i \delta(\mathbf{x} - \mathbf{x}_i), \quad (2)$$

where  $e_i$  is the energy of the  $i$ th particle. In addition, since the energy current,  $j_{ik}$ , between particles  $i$  and  $k$  flows between  $x_k$  and  $x_i$  instead of between their lattice sites, the spatial integral of  $j_{ik}$  (used in the Green-Kubo formula) is also different.

In view of the obvious approximations in the lattice current, is it merely something that works well for stiff crystals? When computing the conductivity from equilibrium correlation functions, are the two currents equivalent in the thermo-

dynamic limit [4]? This would not be sufficient for small structures that are specially designed and cannot be scaled up, for which the conductance has to be used instead of the conductivity [5,6]. Even for large systems, one has to be careful in proving the equivalence of the two currents if the transport coefficients are singular, since the thermodynamic limit of the conductivity does not exist.

Surprisingly, despite the approximations in the lattice current, one can prove an exact Green-Kubo-like formula with it for the conductivity of a finite chain which has Langevin baths attached to the terminal particles [7], using the steady-state fluctuation theorem [8]. This result has been proved without the fluctuation theorem and generalized to a number of different implementations of heat baths [9]. The proof applies to a chain with arbitrary onsite and interparticle potentials (which may vary down the chain, even though the proof does not state this). Therefore, it applies to a tethered or free chain and (by a simple transformation that we shall show in this paper) a chain at constant pressure. Is this agreement accidental, and can the proof of Ref. [7] be extended to the (exact) continuum current as well?

In this paper, we explain the result by obtaining an interpretation of the dynamics of the oscillator chain for which the lattice current is exact; in this interpretation, the Langevin baths are at fixed locations. We further show through analytical and numerical calculations on such a chain that the conductivities obtained using the lattice and continuum currents are not equivalent except in the thermodynamic limit. The ratio of the two differs from unity by  $\sim 1/N$  for a chain with  $N$  particles that is tethered at both ends. For a chain maintained at constant pressure, the approach to unity is slower. If fit to a  $\sim 1/N^\eta$  form, it is consistent with any  $\frac{1}{2} < \eta < 1$ . Our numerics also show that slight changes in the definition of the continuum heat current, which is a linear combination of the energy and particle currents, can markedly change the error in the resultant conductivity; these differences are inconsequential in the thermodynamic limit. The conductivities obtained from lattice and continuum currents are generally very close for  $N \geq 256$ .

One can try to explain the error in the Green-Kubo formula using the continuum current by noting that the size of the system fluctuates in the continuum interpretation. In the tethered case, the terminal particles are adjacent to the tethering posts and the percentage fluctuations in the length are

$\sim 1/N$ , while for a chain at constant pressure they are  $\sim 1/\sqrt{N}$ . This expectation is only partly borne out by the numerics. Note that, in view of the proof in Refs. [7,9], it is the *lattice* current that gives the heat conductivity accurately.

The rest of this paper is organized as follows: Sec. II reviews the derivation of the lattice and continuum heat currents and shows how the lattice heat current is not an approximation if the oscillator dynamics are interpreted suitably. Section III calculates the ratio of the conductivities obtained with the continuum and lattice currents and how they behave as the thermodynamic limit is approached. Section IV presents numerical results with the same for a tethered chain and a chain at constant pressure.

## II. TRANSVERSE AND LONGITUDINAL INTERPRETATIONS

We consider a one-dimensional (1D) chain of particles with nonlinear springs connecting adjacent particles. (The definitions in this section are standard [10], but we include them for clarity.) The Hamiltonian is

$$H = \sum_{i=1}^N \frac{1}{2} m v_i^2 + \sum_{i=1}^{N-1} U(x_{i+1} - x_i) + \sum_{i=1}^N U_0(x_i), \quad (3)$$

where  $m_i$ ,  $x_i$ , and  $v_i$  are the mass, position, and velocity of the  $i$ th particle and  $U$  is the interparticle potential.  $U_0$  is an onsite potential for each particle. When  $U_0=0$ , this is a Fermi-Pasta-Ulam (FPU) chain [11]. The dynamics of this system are Hamiltonian, with heat baths connected to the first and last particle through the addition of Langevin damping  $-\gamma v_{1,N}$  and noise  $\eta_{1,N}(t)$  terms in their equations of motion. As with other one-dimensional systems in which interparticle interactions are momentum conserving [12,13], the FPU chain has a singular heat conductivity, with the thermal conductivity of the chain growing as  $\sim N^{1/3}$  as a function of chain length [13–16]. In higher dimensions or if  $U_0 \neq 0$ , the singularity in the heat conductivity is eliminated.

If we associate the kinetic energy of each particle with itself, and the potential energy of each spring as being equally distributed between its two neighbors, the rate of change in the energy of particle  $i$

$$\dot{e}_i = \frac{1}{2} m v_i^2 + U_0(x_i) + \frac{1}{2} [U(x_{i+1} - x_i) + U(x_{i-1} - x_i)] \quad (4)$$

is

$$\dot{e}_i = m_i v_i \dot{v}_i + U_0'(x_i) v_i + \frac{1}{2} F_{i,i-1} (v_{i-1} - v_i) + \frac{1}{2} F_{i,i+1} (v_{i+1} - v_i), \quad (5)$$

where  $F_{i,i-1}$  is the force on the  $i$ th particle from the  $i-1$ th particle. (There is only one  $F$  term in  $e_1$  and  $e_N$ .) Using the equations of motion, this is equal to

$$\begin{aligned} \dot{e}_i &= \frac{1}{2} F_{i,i-1} (v_{i-1} + v_i) + \frac{1}{2} F_{i,i+1} (v_{i+1} + v_i) \\ &\quad + \delta_{i,1} (-\gamma v_1 + \eta_1) v_1 + \delta_{i,N} (-\gamma v_N + \eta_N) v_N. \end{aligned} \quad (6)$$

Therefore the continuum energy current is

$$\begin{aligned} j_E^c(x, t) &= \sum_{i=1}^N e_i v_i \delta[x - x_i(t)] \\ &\quad + \frac{1}{2} \sum_{i=2}^N F_{i,i-1} (v_{i-1} + v_i) \theta(x - x_{i-1}) \theta(x_i - x), \end{aligned} \quad (7)$$

where the first term comes from the advective transport of the energy associated with each particle by it. Integrating, the energy current flowing through the entire system is

$$J_E^c(t) = \sum_{i=1}^N e_i v_i + \frac{1}{2} \sum_{i=2}^N F_{i,i-1} (v_{i-1} + v_i) (x_i - x_{i-1}). \quad (8)$$

With other choices of how the potential energy of each spring is distributed, this expression can change by small amounts. This result can easily be generalized to higher dimensions

$$J_E^c(t) = \sum_{i=1}^N e_i \mathbf{v}_i + \frac{1}{4} \sum \sum \mathbf{F}_{ik} \cdot (\mathbf{v}_k + \mathbf{v}_i) (\mathbf{x}_i - \mathbf{x}_k). \quad (9)$$

On the other hand, if the springs between the particles are very stiff, each particle only deviates slightly from its lattice position. If we neglect the advective term in the heat current and approximate  $x_i \approx ia$  (where  $a$  is the lattice constant), we obtain an energy current equal to  $F_{i,i-1} (v_{i-1} + v_i)$  between the  $i-1$ th and  $i$ th lattice sites, which integrates to the lattice energy-current

$$J_E^l(t) = \frac{1}{2} \sum_{i=2}^N F_{i,i-1} (v_{i-1} + v_i) a. \quad (10)$$

The generalization to higher dimensions is again straightforward. For a one-dimensional system, in which the ordering of particles is fixed, it is always possible to view the positions of the particles as displacements from a reference lattice, but in higher dimensions this is only useful in a crystal-line phase.

By its construction, the lattice energy-current  $J_E^l$  seems clearly an approximation; if a Green-Kubo-like formula exists for finite oscillator chains, one would expect it to be only approximate if the lattice current is used. Despite this, one can prove an exact Green-Kubo-type formula for finite oscillator chains with Langevin baths if the lattice current is used [7]:

$$\kappa = \frac{1}{k_B T^2 (N-1) a} \int_0^\infty \langle J_Q(t) J_Q(0) \rangle dt. \quad (11)$$

In Eq. (11)  $J_Q(t)$  is the spatially integrated heat current (defined in the next section) flowing at time  $t$  through the chain of  $N$  particles at a temperature  $T$ .

As mentioned in the previous section, one can construct an interpretation of the oscillator-chain dynamics for which the lattice current is exact. Let  $x_i = ia + \zeta_i$ , where  $\zeta_i$  is the displacement of the  $i$ th particle from its lattice position. We imagine that the displacement is transverse to the chain instead of along it. If the potential between neighboring particles is expressed as  $U(\zeta_{i+1} + a - \zeta_i)$ , the dynamics are the same as if the displacements  $\zeta_i$  had been in the longitudinal

direction. The energy current flowing into the Langevin baths is also unchanged. In this interpretation, the spatially integrated energy current is  $J_E^l$  with no approximations [17]: there is no advective term in the current, and the energy current between neighboring particles flows over a distance  $a$  instead of  $x_i - x_{i-1} = a + \zeta_i - \zeta_{i-1}$ . (The transverse interpretation is in fact more natural for the often-studied “phantom” oscillator chains, where particles can pass through each other but only neighboring lattice sites interact.)

Since the lattice and continuum currents are exact for the transverse and longitudinal interpretations, respectively, and the heat flowing between the reservoirs is independent of interpretation, one might hope that Eq. (11) would be valid for both currents. In the rest of this paper, we shall show that this is not the case except in the thermodynamic limit.

### III. LATTICE AND CONTINUUM HEAT CURRENTS

The proof in Ref. [7] uses the lattice energy current for the heat current for a system at zero pressure. Applying pressure at the ends of the chain is equivalent to replacing  $U(x_i - x_{i-1})$  with  $U(x_i - x_{i-1}) - p(x_i - x_{i-1})$ . From Eq. (10), this changes the heat current to

$$J_Q^l(t) = \frac{1}{2} \sum_{i=2}^N [F_{i,i-1} - p](v_{i-1} + v_i)a, \quad (12)$$

with which definition the proof of Ref. [7] is extended to systems at nonzero pressure. The heat current in the continuum interpretation is defined through Galilean invariance as [3,18]

$$J_Q^c(t) = J_E^c(t) - [E + (N-1)pa]v_{CM}, \quad (13)$$

where  $E$  is the time average of the energy of the system and  $v_{CM}$  is the instantaneous velocity of the center of mass defined by

$$v_{CM} = \frac{1}{N} \sum_{i=1}^N v_i = \frac{1}{N} J_N, \quad (14)$$

where  $J_N$  is the number current.

In comparing  $J_Q^c$  and  $J_Q^l$ , it is useful to first derive an identity that is valid for the autocorrelation function of any conserved current

$$\begin{aligned} \int_0^\infty C(t) dt &= \lim_{\tau \rightarrow \infty} \frac{1}{2\tau} \int_0^\tau \int_0^\tau \langle \mathbf{J}(t_1) \cdot \mathbf{J}(t_2) \rangle dt_1 dt_2 \\ &= \lim_{\tau \rightarrow \infty} \frac{1}{2} \left\langle \left[ \frac{1}{\sqrt{\tau}} \int_0^\tau \mathbf{J}(t) dt \right]^2 \right\rangle. \end{aligned} \quad (15)$$

Thus, in Eq. (11), we are interested in the  $O(\sqrt{\tau})$  part of  $\int_0^\tau \mathbf{J}_Q(t) dt$ . In particular, in Eq. (12) we have

$$\frac{1}{2} p \sum_{i=2}^N (v_{i-1} + v_i)a \equiv (N-1)pa v_{CM} \quad (16)$$

similar to Eq. (13), since  $\int_0^\tau [v_i(t) - v_{CM}(t)] dt$  is equal to the change in  $x_i(t) - x_{CM}(t)$ , which cannot be  $O(\sqrt{\tau})$ . Note that

even though  $J_Q(t)$  has a power-law tail to its autocorrelation function, this tail is cut-off for large time for any finite  $N$ , as it *must* be from Eq. (15) if the thermal conductivity is to be finite for that  $N$ .

As another useful result, if  $\rho$  is the charge density corresponding to a current  $\mathbf{j}_\rho$ , then

$$\begin{aligned} \frac{d}{dt} \int \mathbf{x} \rho(\mathbf{x}, t) d\mathbf{x} &= - \int \mathbf{x} \nabla \cdot \mathbf{j}_\rho(\mathbf{x}, t) d\mathbf{x} \\ &= - \int_S \mathbf{x} \mathbf{j}_\rho(\mathbf{x}, t) \cdot d\mathbf{S} + \mathbf{J}_\rho(t), \end{aligned} \quad (17)$$

in which the integral on the right-hand side is over the surface of the system, where it is connected to reservoirs.

#### A. Tethered chain

Let the FPU chain of Eq. (3) be tethered at the ends. This is accomplished by adding extra fixed particles at the zeroth and  $N+1$ th locations with springs connecting them to their neighbors. With these boundary conditions, the displacement of the center of mass in a time interval  $\tau \rightarrow \infty$  must be  $O(1)$ . Then from Eq. (15), the energy and heat currents yield the same result in Eq. (11), both for the lattice and continuum currents.

From the continuity equation,

$$\begin{aligned} \frac{d}{dt} \sum (i-1)ae_i(t) &= - \int_0^{(N-1)a} (y-a) \frac{dj_E^l(y,t)}{dy} dy \\ &= J_E^l(t) - (N-1)aJ_{E,R}(t), \end{aligned} \quad (18)$$

where  $y$  is a continuous coordinate along the lattice, such that  $j_E^l(y)$  is piecewise constant with discontinuities at integer multiples of the lattice-constant  $a$ .  $J_{E,R}(t)$  is the energy current flowing into the heat bath at the right end of the system. If we integrate both sides of this equation over an extremely large time-interval  $\tau$ , the left-hand side does not diverge with  $\tau$ . The first term on the right-hand side must be  $O(\sqrt{\tau})$  from Eq. (15), and therefore so must be the second term. Keeping only terms that grow as  $O(\sqrt{\tau})$ , we obtain

$$\int_0^\tau J_E^l(t) dt \equiv (N-1)a \int_0^\tau J_{E,R}(t) dt. \quad (19)$$

Similarly, since from Eq. (15) the left-hand side of Eq. (19) is  $O(N^{(1+\alpha)/2})$  for large  $N$  where  $\alpha$  is the heat-conductivity exponent [10], the right-hand side must be the same.

We can try to understand the  $O(\sqrt{\tau}N^{(1+\alpha)/2})$  scaling of the right-hand side as follows: on extremely long-time scales,  $J_{E,R}(t)$  is as likely to be negative as positive. Thus, the right-hand side of Eq. (19) is  $O(\sqrt{\tau})$  for large  $\tau$ . On the other hand, if energy flows into the system from the reservoir to the right, it increases the local energy density, thereby increasing the likelihood that energy will flow out shortly afterwards. As  $N \rightarrow \infty$ , all the energy that flows in from the reservoir to the right must eventually flow out to the same reservoir instead of escaping to the left. Consequently,  $J_{E,R}(t)$  is anticorrelated up to a time scale that diverges with  $N$ . This reduces the  $O(N)$  dependence one might naively expect for the right-

hand side of Eq. (19). Although the arguments in this paragraph are qualitative, the  $O(\sqrt{\tau}N^{(1+\alpha)/2})$  scaling of the right-hand side of Eq. (19) is derived rigorously in the previous paragraph.

For the continuum energy current,

$$\begin{aligned} \frac{d}{dt} \sum e_i(t)x_i &= \frac{d}{dt} \int_{x_1(t)}^{x_N(t)} e(x,t)xdx \\ &= - \int x \frac{dj_E^c(x,t)}{dx} dx \\ &= J_E^c(t) + x_1(t)J_{E,L}(t) - x_N(t)J_{E,R}(t), \end{aligned} \quad (20)$$

where  $J_{E,L}$  is the heat current flowing out of the reservoir on the left-hand side of the system. With  $x_{1,N}(t)=[0, (N-1)a] + \zeta_{1,N}(t)$

$$\begin{aligned} \int_0^\tau J_E^c(t)dt &\equiv (N-1)a \int_0^\tau J_{E,R}(t)dt \\ &+ \int_0^\tau [\zeta_N(t)J_{E,R}(t) - \zeta_1(t)J_{E,L}(t)]dt. \end{aligned} \quad (21)$$

Compared to Eq. (19), the extra term on the right-hand side is also  $O(\sqrt{\tau})$  for large  $\tau$ . However, the missing factor of  $(N-1)$  makes it negligible compared to the first term in the thermodynamic limit.

One would expect the factors of  $\zeta$  in the integrand to destroy the temporal anticorrelation of  $J_{E,L}$  and  $J_{E,R}$  so that the last term should be independent of  $N$ . Thus, we would expect

$$\frac{\int_0^\infty C_{QQ}^c(t)dt}{\int_0^\infty C_{QQ}^l(t)dt} - 1 \sim N^{-(1+\alpha)} \sim N^{-4/3}. \quad (22)$$

Contrary to this expectation, we will see numerically that the right-hand side is in fact proportional to  $1/N$ , as suggested in Sec. I. We must conclude that the correlations between  $\zeta$  and  $J_{E,L,R}$  are more subtle than one would naively expect.

### B. Constant pressure boundary conditions

If the FPU chain has a constant pressure  $p$  applied to it instead of being tethered at the ends, the equivalence of the continuum and lattice heat currents is more delicate. The tethering is removed, and the pressure effectively adds a term  $p(x_N - x_1)$  to the potential energy in Eq. (3). The center of mass of the system executes a random walk due to the fluctuating forces exerted by the heat baths, moving a distance  $O(\sqrt{\tau})$  in time  $\tau$ . The volume of the system also fluctuates by  $O(\sqrt{N})$ . However, the lattice description is essentially the same as for the tethered chain. Since the system at a pressure  $p$  is equivalent to a system at zero pressure with an extra  $p(x_i - x_{i-1})$  in the interparticle energy, from Eq. (12) the continuity equation Eq. (18) is modified to

$$\begin{aligned} \frac{d}{dt} \sum (i-1)a \left[ e_i(t) + \frac{1}{2}pa(x_i - x_{i-1}) + \frac{1}{2}pa(x_{i+1} - x_i) \right] \\ = J_E^l(t) - pa \sum_{i=2}^N \frac{1}{2}(v_i + v_{i-1}) - (N-1)aJ_{E,R}(t), \end{aligned} \quad (23)$$

from which

$$\int_0^\tau J_Q^l(t)dt \equiv (N-1)a \int_0^\tau J_{E,R}(t)dt \quad (24)$$

as before. Note that we could have used  $(i-1-k)a$  on the left-hand side of Eq. (23), which would have yielded a linear combination of  $J_{E,R}(t)$  and  $J_{E,L}(t)$  on the right-hand side of Eq. (24).

Turning to the continuum current,

$$\begin{aligned} \frac{d}{dt} \sum e_i(t)x_i &= J_E^c(t) + x_1J_{E,L}(t) - x_NJ_{E,R}(t) \\ &+ px_1 \frac{dx_1}{dt} - px_N \frac{dx_N}{dt}, \end{aligned} \quad (25)$$

where on the right-hand side we have included the energy current from the reservoirs and the work done by the applied pressure. We define the heat current (integrated over the chain) as

$$J_Q^c(t) = J_E^c(t) - \{E(t) + p[x_N(t) - x_1(t)]\}v_{CM}, \quad (26)$$

where  $E(t)$  is the total energy of the system at time  $t$  and  $v_{CM}$  is the velocity of the center of mass. This definition is slightly different from that in Eq. (13); if  $E(t)$  and  $x_N(t) - x_1(t)$  are replaced with their average values, we recover the earlier expression. We also use conservation of energy

$$\frac{dE(t)}{dt} = J_{E,L}(t) - J_{E,R}(t) + p \frac{dx_1}{dt} - p \frac{dx_N}{dt}. \quad (27)$$

Multiplying this equation by  $x_{CM}$ , subtracting from Eq. (25) and using Eq. (26), we have

$$\begin{aligned} \frac{d}{dt} \sum e_i(t)[x_i - x_{CM}] \\ = J_Q^c(t) + (x_1 - x_{CM})J_{E,L}(t) - (x_N - x_{CM})J_{E,R}(t) \\ + p(x_1 - x_{CM}) \frac{d}{dt}(x_1 - x_{CM}) - p(x_N - x_{CM}) \frac{d}{dt}(x_N - x_{CM}). \end{aligned} \quad (28)$$

Therefore,

$$\begin{aligned} \int_0^\tau J_Q^c(t)dt &\equiv \frac{1}{2}(N-1)a \int_0^\tau [J_{E,R}(t) + J_{E,L}(t)]dt \\ &+ \int_0^\tau (\zeta_N - \zeta_{CM})J_{E,R}(t)dt \\ &+ \int_0^\tau (\zeta_{CM} - \zeta_1)J_{E,L}(t)dt. \end{aligned} \quad (29)$$

As per the discussion after Eq. (24), the first term on the right-hand side is equivalent to  $\int_0^\tau J_Q^l(t) dt$ . As per the discussion after Eq. (19), this is  $\sim \sqrt{\tau N^{1+\alpha}}$ . The last two terms are also proportional to  $\sqrt{\tau}$ . Unlike for the tethered case, since  $\zeta_{1,N} - \zeta_{CM}$  is  $O(\sqrt{N})$ , it is not clear they can be neglected even in the thermodynamic limit. Therefore, to compare the lattice and continuum conductivities with constant pressure boundary conditions, we turn to numerical simulations in the next section. Note that if we had used the first definition of the heat current, Eq. (13), Eq. (29) would have had an extra term on the right-hand side

$$\int_0^\tau [E - E(t) - p\zeta_N(t) + p\zeta_1(t)] v_{CM}(t) dt, \quad (30)$$

with which it is even less clear that the lattice and continuum results are equivalent.

#### IV. NUMERICAL RESULTS

In the numerical simulations we set the on-site potential  $U_0(x)$  in Eq. (3) to be zero, and take the interparticle potential to be

$$U(x_{i+1} - x_i) = \frac{1}{2}(\zeta_{i+1} - \zeta_i)^2 + \frac{w}{3}(\zeta_{i+1} - \zeta_i)^3 + \frac{u}{4}(\zeta_{i+1} - \zeta_i)^4, \quad (31)$$

where  $\zeta_i = x_i - ia$ . The lattice spacing  $a$  is taken to be unity. We consider  $N$  particles of which the first and last are coupled to heat baths at temperature  $T$ . Each particle in the interior interacts with neighbors to the left and to the right, while the first and last particles only interact with one neighbor. These end particles have additional forces due to the friction and noise,  $-\gamma v_1 + \eta_1$  and  $-\gamma v_N + \eta_N$ . In the tethered chain, particles 1 and  $N$  also interact with an extra tethered ‘‘particle’’ at the zeroth and  $N+1$ th sites, respectively. In the constant pressure chain, particles 1 and  $N$  feel an extra inward force, equal to the pressure  $p$ . The noise satisfies the fluctuation-dissipation theorem  $\langle \eta_i(t) \eta_j(t') \rangle = 2k_B T \gamma \delta(t-t') \delta_{ij}$ .

We integrated the equations of motion using the second-order velocity Verlet (leapfrog) method for all particles in the interior. For those on the boundary, which are coupled to the heat baths and so subjected to random noise, we just used the simple Euler method, so, for example, for particle 1,

$$v_1(t + \delta t) = v_1(t) + F(\zeta_1 - \zeta_2) \delta t - \gamma v_1(t) \delta t + R \epsilon(t), \quad (32)$$

where the force,  $F(\zeta_1 - \zeta_2)$ , is equal to  $-dU/d\zeta_1$  with  $U$  given by Eq. (31), and  $\epsilon$  is a Gaussian random variable with mean 0 and standard deviation unity. The coefficient of the noise,  $R$ , is the root-mean-square fluctuation in the noise integrated over time  $\delta t$ , so it is given by

$$\begin{aligned} R^2 &= \int_0^{\delta t} dt \int_0^{\delta t} dt' \langle \eta(t) \eta(t') \rangle \\ &= \int_0^{\delta t} dt \int_0^{\delta t} dt' 2k_B T \gamma \delta(t-t') \\ &= 2k_B T \gamma \delta t. \end{aligned} \quad (33)$$

We focused on one set of parameters,  $w=0.5$ ,  $u=1.0$ ,  $\gamma=0.5$ , and  $T=k_B=1.0$ , and for the constant pressure simulations we took  $p=0.1$ .

We start the system off with all velocities equal to zero, and the particles separated by their equilibrium distance  $a$ , so all the energy is fed in from the baths at the boundaries. We run for a time  $t_{\text{equil}}$  to equilibrate, and then continue for an additional time  $t_{\text{meas}}$  during which measurements of the current are made after every time step. This whole process, both equilibrating and averaging, is then repeated  $n_{\text{run}}$  times and the results averaged. Error bars are estimated from the standard deviation of results from different runs in the usual way. The values of the parameters used are given in Table I. The thermal conductivity is obtained from the simulations from

$$\kappa = \frac{1}{2(N-1)T^2 t_{\text{meas}}} \left\langle \left[ \int_0^{t_{\text{meas}}} J_Q(t_{\text{equil}} + t) dt \right]^2 \right\rangle, \quad (34)$$

where  $\langle \dots \rangle$  denotes the average over the  $n_{\text{run}}$  runs.

We investigated the size dependence of the difference between the thermal conductivities calculated with the continuum currents, Eqs. (13) and (26), from that obtained with the lattice current, Eq. (12). This difference is always small, and, especially for the tethered chain simulations, depends sensitively on the time step,  $\delta t$ . We shall therefore present results as a function of both  $\delta t$  and  $N$ . As discussed at the start of Sec. I, for a tethered chain in which the heat current is defined by Eq. (13), the terms subtracted from the energy current are inconsequential for the conductance.

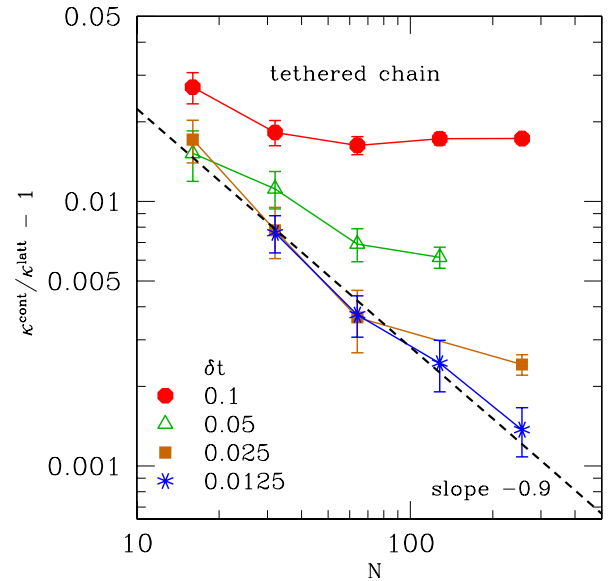


FIG. 1. (Color online) Results for the tethered chain. A log-log plot of the ratio of the continuum thermal conductivity with the heat current defined in Eq. (13) to the lattice thermal conductivity with the heat current defined in Eq. (12), minus one. If the continuum and lattice thermal conductivities agree in the thermodynamic limit, the results should tend to zero for  $N \rightarrow \infty$ . The best fit has a slope of  $-0.9$ , close to  $-1$  instead of  $-4/3$ , which is explained near the end of Sec. I.

TABLE I. Parameters of the tethered chain simulations for different values of particle-number  $N$  and time-step  $\delta t$ .  $t_{\text{equil}}$  is the time for equilibration,  $t_{\text{meas}}$  is the subsequent time during which measurements are performed, and  $n_{\text{run}}$  is the number of “runs,” where one run comprises the equilibration plus the measurement time steps.

$N$	$\delta t$	constant $V$			constant $p$		
		$t_{\text{equil}}$	$t_{\text{meas}}$	$n_{\text{run}}$	$t_{\text{equil}}$	$t_{\text{meas}}$	$n_{\text{run}}$
16	0.10	25000	50000	4000	25000	50000	4000
16	0.05	25000	50000	4000	25000	50000	4000
16	0.025	25000	50000	4000	25000	50000	4000
16	0.0125				25000	50000	4000
32	0.10	50000	100000	4000	50000	100000	4000
32	0.05	50000	100000	4000	50000	100000	4000
32	0.025	50000	100000	4000	50000	100000	4000
32	0.0125	100000	200000	8000	50000	100000	4000
64	0.10	100000	200000	4000	100000	200000	4000
64	0.05	100000	200000	4000	100000	200000	4000
64	0.025	100000	200000	4000	100000	200000	4000
64	0.0125	200000	400000	8000	100000	200000	4000
128	0.10	200000	400000	4000	200000	800000	4000
128	0.05	200000	400000	4000	200000	800000	4000
128	0.025	200000	400000	4000	200000	800000	4000
128	0.0125	400000	800000	4000	200000	800000	4000
256	0.10	500000	1000000	4000	500000	1000000	4000
256	0.05				300000	600000	8000
256	0.025	1000000	2000000	4000	500000	1000000	4000
256	0.0125	1000000	2000000	4000	1000000	2000000	4000

**A. Tethered chain**

Figure 1 presents data for the tethered chain for the ratio of the thermal conductivity from the continuum current in Eq. (13) to that from the lattice current in Eq. (12), minus 1, as a function of system-size  $N$ , for different values of the time-step  $\delta t$ . If the continuum and lattice thermal conductivities agree in the thermodynamic limit, the results should tend to zero for  $N \rightarrow \infty$ . It is clearly essential to extrapolate the results to small values of  $\delta t$ , and when one does so, the result is close to the expected  $1/N$  dependence. The best fit of the data for the smallest value of  $\delta t$  gives  $1/N^\eta$  with  $\eta \approx 0.9$ , but the small difference in the value of the exponent  $\eta$  from one is probably due to corrections to scaling which are not completely negligible for this range of sizes.

In Fig. 2 we show data similar to Fig. 1, but using the second definition of the continuum current, in Eq. (26). The difference in thermal conductivities is smaller, so it is harder to get good statistics on it, but it also seems to decay with size like  $1/N$ . This conclusion disagrees with the naive expectation of Eq. (22), but is consistent with the physical argument given in the introduction.

**B. Constant pressure chain**

For the constant pressure chain, Fig. 3 plots the ratio of the thermal conductivity using the continuum heat current in

Eq. (13) to that using the lattice current in Eq. (12), minus 1. For reasons that are not clear to us, the dependence on time step is much smaller than for the corresponding tethered chain results in Fig. 1. A fit to the data gives a size depen-

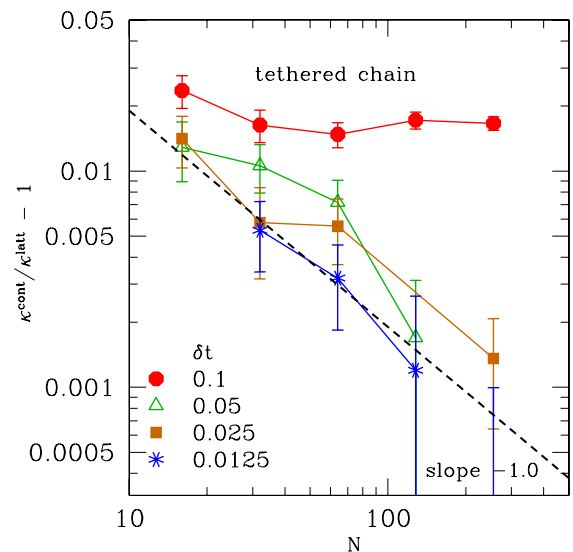


FIG. 2. (Color online) Results for the tethered chain. A log-log plot of same as for Fig. 1, but using the continuum heat current given by Eq. (26).

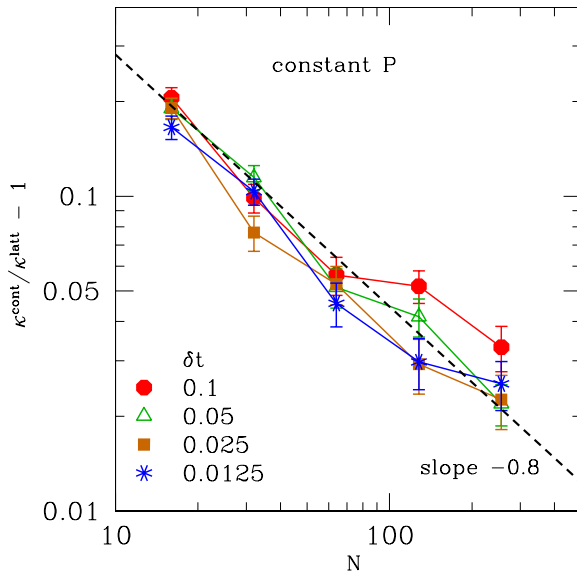


FIG. 3. (Color online) Results for the constant pressure chain. A log-log plot of the ratio of the continuum thermal conductivity with the heat current defined in Eq. (13) to the lattice thermal conductivity with the heat current defined in Eq. (12), minus one. The best fit has a slope of about  $-0.8$ .

dence of  $N^{-\eta}$  with  $\eta \approx 0.8$ . Taken naively, this is a faster decay than the  $1/N^{1/2}$  dependence expected for constant pressure, as discussed in the introduction. However, the error bars on the exponent are sufficiently large that any  $1 > \eta > \frac{1}{2}$  is possible. It is also possible that larger sizes are needed to see the asymptotic size dependence. We note that the relative uncertainty in the length of the system is of order  $1/N^{1/2}$  and it seems surprising to us that difference in thermal conductivities could be smaller than this asymptotically. Despite these uncertainties, the relative difference in thermal conductivities is small, even for constant pressure, and appears to vanish in the thermodynamic limit.

Finally, Fig. 4 is similar to Fig. 3 but uses the alternative definition of the head current in Eq. (26). There is still a nonzero difference compared with the lattice conductivity but it is smaller, so the error bars are larger, as a result of which it is not possible to reliably estimate any functional form for the difference.

## V. CONCLUSION

In this paper, we have shown that the continuum and lattice versions of the heat current yield different results

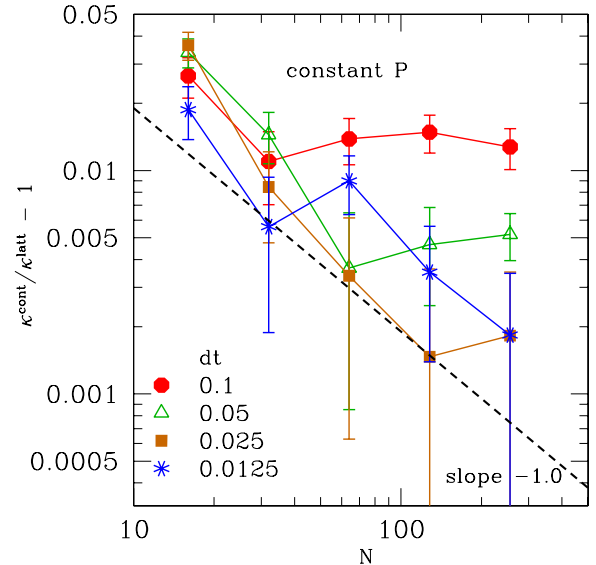


FIG. 4. (Color online) Results for the constant pressure chain. A log-log plot of same as Fig. 3 but using the continuum heat current given in Eq. (26). The error bars are sufficiently large that it is not possible to estimate the size dependence reliably.

for the heat conductivity of a finite oscillator chain with Langevin baths through the Green-Kubo formula. The results using the continuum and lattice currents are different for a finite chain. Since the thermal conductivity obtained using the lattice current is exact [7], this implies that results using the continuum current are approximate even though this current is apparently exact. Numerically, if the error is fit to a form  $\sim 1/N^\eta$  for a chain of  $N$  particles, we obtain  $\eta \lesssim 1$  for a chain that is tethered just beyond its end points. We can argue that the error is at least partly because the length of the chain fluctuates, and therefore must be bounded below by  $\sim 1/N$ ; our numerical results are close to and slightly above this lower bound. The same argument would yield a lower bound to the error of  $\sim 1/\sqrt{N}$  for a chain at constant pressure. Surprisingly, though, the numerical results for such a chain show an error that decays *faster*, almost as  $1/N$ , although the asymptotic large  $N$  exponent may approach 0.5. A small change in the definition of the continuum heat current, which is benign in the thermodynamic limit, reduces the error substantially.

- [1] R. Kubo, J. Phys. Soc. Jpn. **12**, 570 (1957); R. Kubo, M. Yokota, and S. Nakajima, *ibid.* **12**, 1203 (1957).
- [2] J. M. Luttinger, Phys. Rev. **135**, A1505 (1964).
- [3] D. Forster, *Hydrodynamic Fluctuations, Broken Symmetry, and Correlation Functions* (Addison Wesley, Indiana, Lebanon, 1975).
- [4] It is easy to prove that the time average of the two currents is

- the same when a small temperature difference is applied across the system. Here we are considering the conductivity as obtained from the equilibrium correlations. As discussed later in the paper, this involves calculating the  $\sim O(\sqrt{\tau})$  fluctuations in the current integrated over a time  $\tau$ , which is more delicate than the  $O(\tau)$  part of the out-of-equilibrium integral.
- [5] P. A. Lee and D. S. Fisher, Phys. Rev. Lett. **47**, 882 (1981).

- [6] A. Szafer and A. D. Stone, IBM J. Res. Dev. **32**, 384 (1988).
- [7] L. Rey-Bellet and L. E. Thomas, Ann. Henri Poincaré **3**, 483 (2002); D. Andrieux and P. Gaspard, J. Stat. Mech.: Theory Exp. (2007), P02006.
- [8] G. Gallavotti and E. G. D. Cohen, Phys. Rev. Lett. **74**, 2694 (1995); G. Gallavotti, *ibid.* **77**, 4334 (1996).
- [9] A. Kundu, A. Dhar, and O. Narayan, J. Stat. Mech.: Theory Exp. (2009), L03001.
- [10] S. Lepri, R. Livi, and A. Politi, Phys. Rep. **377**, 1 (2003).
- [11] E. Fermi, J. Pasta, and S. Ulam, in, Los Alamos Scientific Laboratory Report No. LA-1940, 1955 (unpublished).
- [12] T. Prosen and D. K. Campbell, Phys. Rev. Lett. **84**, 2857 (2000).
- [13] O. Narayan and S. Ramaswamy, Phys. Rev. Lett. **89**, 200601 (2002).
- [14] P. Grassberger, W. Nadler, and L. Yang, Phys. Rev. Lett. **89**, 180601 (2002); G. Casati and T. Prosen, Phys. Rev. E **67**, 015203(R) (2003); J. M. Deutsch and O. Narayan, *ibid.* **68**, 041203 (2003); P. Cipriani, S. Denisov, and A. Politi, Phys. Rev. Lett. **94**, 244301 (2005); T. Mai and O. Narayan, Phys. Rev. E **73**, 061202 (2006); T. Mai, A. Dhar, and O. Narayan, Phys. Rev. Lett. **98**, 184301 (2007).
- [15] S. Lepri, R. Livi, and A. Politi, EPL **43**, 271 (1998); Phys. Rev. E **68**, 067102 (2003); L. Delfini, S. Lepri, R. Livi, and A. Politi, J. Stat. Mech.: Theory Exp. (2007), P02007; Phys. Rev. E **73**, 060201(R) (2006); Phys. Rev. Lett. **100**, 199401 (2008); A. Dhar and O. Narayan, *ibid.* **100**, 199402 (2008).
- [16] B. Li and J. Wang, Phys. Rev. Lett. **91**, 044301 (2003); J. S. Wang and B. Li, *ibid.* **92**, 074302 (2004); J. S. Wang and B. Li, Phys. Rev. E **70**, 021204 (2004).
- [17] In a hydrodynamic description, the displacement of the particles from their lattice positions is a function of the density, which is a conserved quantity in the longitudinal interpretation; in the transverse interpretation it is a broken symmetry (even though there is no long-range order in the chain). Therefore in both interpretations, the displacement is associated with a hydrodynamic variable, though the cause is different.
- [18] R. Kubo, *Statistical Mechanics* (North Holland, New York, 1965).